Developmental Neuroscience

Rolf Gruetter
Elizabeth R. Seaquist
Suckwon Kim
Kâmil Uğurbil

Departments of Radiology, Medicine, Psychiatry and Biochemistry, University of Minnesota, Minneapolis, Minn., USA

Localized in vivo ^{13}C-NMR of Glutamate Metabolism in the Human Brain: Initial Results at 4 Tesla

Abstract

Using optimized administration of ^{13}C-labeled glucose, the time course of the specific activity of glucose was measured directly by in vivo ^{13}C-NMR in the human brain at 4 Tesla. Subsequent label incorporation was measured at the C2, C3 and C4 positions of both glutamate and the well-resolved C2, C3 and C4 resonances of glutamine and at the C2 and C3 positions of aspartate. GABA was clearly observed for the first time in vivo, suggesting a substantial GABA turnover in the normal human visual cortex. Likewise, lactate C3 labeled with an estimated active pool size on the order of 0.5 mM. A model of cerebral glutamate metabolism is proposed which predicts that glutamatergic action ('neurotransmission'), pyruvate carboxylase flux, TCA cycle activity, glucose consumption and exchange across the mitochondrial membrane can be assessed simultaneously in the human brain.

Introduction

Glucose is the main substrate used for energy metabolism by the normal human brain. Once transported across the blood-brain barrier, glucose is readily metabolized [1, 2]. Studies of nervous tissue have shown that label from glucose accumulates in the intermediates of glycolysis and of the TCA cycle, as well as in glutamate (Glu), glutamine (Gln), GABA, lactate (Lac), alanine (Ala) and aspartate (Asp) [3–6]. The mechanism for label accumulation was attributed to active exchange reactions between amino acids and TCA cycle intermediates [7, 8]. The major excitatory neurotansmitter Glu [9] is present in the mammalian brain in high concentrations and is dynamically stored in vesicles [10]. To avoid excitotoxic nerve cell damage, the extracellular concentration of Glu must be maintained very low (~ 0.004 mM), which is achieved by efficient high-affinity transport primarily into glia.

Experiments have long suggested that cerebral metabolism is compartmentalized. Early radioisotope studies performed in animal brain between 1950 and 1970 in which an abnormal product-precusor relationship was observed between Glu and Gln led to the conclusion that cerebral metabolism is characterized by at least two compartments that differ by the size of the respective Glu pools [1]. These measurements have been recently extended using ^{13}C-NMR spectroscopy of brain slices [11], extracts [5, 12, 13] and cell cultures [14]. Cellular compartmentation of metabolism has been further supported by the glial localization of Gln synthetase (EC 6.3.1.2) [15], as well as pyruvate carboxylase (EC 6.4.1.1) [16] and by the observation that acetate uptake and metabolism takes place predominantly in astrocytes. In addition, glutaminase (EC 3.5.1.2) activity has been localized predominantly to the neuronal compartment [17]. Morphological evidence suggests that most Gln is normally located in

Rolf Gruetter
Center for MR Research and Clinical Research Center
385 East River Road
Minneapolis, MN 55455 (USA)
Tel. +1 612 626 2435, Fax +1 612 626 7005, E-Mail gruetter@geronimo.drad.umn.edu

astrocytes and glia, whereas Glu is located in the neuronal compartment, most probably in the neuropil [18]. Compartmentation of metabolism may also be present at the level of glycolysis, consistent with a predominantly glial glycolytic activity and oxidative metabolism being predominant in neurons, thus providing a further link between glial energy metabolism and neuronal activation [2]. In summary, most evidence supports the notion that the compartmentalized glial-neuronal metabolic relationship is essential to neurotransmission.

Most of the aforementioned evidence on cerebral metabolism has been derived from studies performed either on cell cultures, brain extracts or on cell preparations. It is unclear to what extent they reflect the physiologic situation present in vivo in the human brain, since several problems may limit the accuracy of these findings: (a) It is known that vesicles containing Glu are docked at the presynaptic membrane and are ready to release Glu almost instantaneously, which may happen during the finite time of any extraction process. (b) Cell cultures, on the other hand, have the drawback that the culturing process can influence gene transcription and protein expression and thereby lead to altered enzyme activities and cells in culture are removed from the important regulatory signals contained within the whole animal. Quantitation of relative activities of metabolic pathways from cell culture may thus not reflect the in vivo situation accurately. (c) Brain slices may have a hypoxic core, the neuronal connections are by design severed and may thus have altered rates of neuronal-glial metabolic trafficking. Finally, (d) fixation studies combined with immunochemical assays provide still images of cerebral compartmentation and do not allow investigation of the dynamic living system.

NMR is a powerful method to study tracer uptake in the in vivo brain [11, 19]. Different approaches and isotopes have been used, such as indirect ^{13}C and ^{15}N detection [20–23]. When using ^{13}C-labeled substrate, direct ^{13}C-NMR detection can be a powerful analytical method to study complex metabolic interactions in cerebral tissue in vitro, in situ and in vivo [4, 24–27]. Cerebral TCA cycle activity [7, 21], mitochondrial exchange [8], malate-aspartate shuttle [28] and pyruvate carboxylase [5] have been studied using ^{13}C-NMR. Extensions of these methods to in vivo brain have been reported by only a few studies [6, 25]. Although ^{13}C signals can in principle be observed using heteronuclear correlation spectroscopy by detecting ^{13}C chemical shift evolution from the attached ^{1}H-, ^{13}C-NMR remains to date the only method that can reliably quantitate distinct signals from all Glu and Gln

carbon positions *noninvasively* in a direct manner. Thus ^{13}C-NMR has excellent potential to study neurochemistry in humans. To date, only one study of cerebral Glu and Gln metabolism using *localized* ^{13}C-NMR has been reported in humans [6]. That study also observed in vivo homonuclear coupling in the glutamate molecule which was observed despite infusion of singly labeled glucose because of subsequent metabolism and label scrambling in the TCA cycle. ^{13}C-NMR has not been easy in vivo because of the increased chemical shift dispersion and inherently low sensitivity. The first proton decoupled ^{13}C-NMR of the human *head* was reported at 1.5 Tesla [29], which showed amidst the presence of dominant lipid signals, glucose and glutamate resonances during 99% glucose infusions. Using higher order shimming and three-dimensional localization methods, a study quantified *localized* glucose signals in the human *brain* at 2.1 Tesla using 50% enriched infusions [30]. Most recently, these studies were extended to the measurement of brain glucose using *natural abundance* ^{13}C-NMR at 4 Tesla [31]. The time courses of Glu and Gln labeling during ^{13}C glucose infusions reported in Gruetter et al. [6] were modeled to derive cerebral metabolic rates which provided the first assessment of cerebral glutamine turnover rates in humans [7]. The present study extends these observations to the simultaneous, but separate observation of all CH$_n$, i.e. proton bound, carbon resonances of Glu and Gln. To achieve the necessary sensitivity, several limitations of ^{13}C-NMR had to be overcome, namely the low sensitivity, the demands on localization due to the large chemical shift displacement error and broadband decoupling. Some of these achievements have been recently described, based on natural abundance detection of many metabolites [31–33].

It was the purpose of this study to further demonstrate that in conjunction with ^{13}C-labeled substrate such as 1-^{13}C glucose, most of the technical obstacles to routinely study human brain (and thus also animal brain) in vivo with ^{13}C-NMR can be overcome. In addition, we propose a simplified model describing glial-neuronal metabolism and test some of its predictions on the in vivo data obtained from the human brain.

Materials and Methods

A total of 4 subjects were studied after giving informed consent according to procedures approved by the Institutional Review Board. On the morning of study, the subject reported to the Center for Magnetic Resonance Research in the fasting state. In preparation for the clamp procedure, an intravenous catheter was placed antegrade in

each forearm and retrograde into a foot. The extremity into which a catheter was placed was warmed by preheated pads to arterialize the venous blood [34]. Somatostatin was infused into one arm vein at a progressively increasing rate up to 0.16 µg/kg/min to suppress endogenous pancreatic insulin and glucagon secretion [35]. 30 g of 99% enriched 1-[13]C D-glucose (50% weight/volume; Isotech, Miamisburg, Ohio, USA) was infused into the other arm vein using a bolus infusion over 2–5 min. 70% 1-[13]C D-glucose was infused thereafter at a variable rate adjusted to maintain target glycemia above 10 mM. Alterations in the glucose infusion rate were made based on the plasma glucose concentration measured on a nearby blucose analyzer (Beckman, Fullerton, Calif., USA) in blood samples taken from the foot vein every 3–5 min.

All studies used a 4 Tesla magnet with a 125-cm bore, equipped with a standard clinical body gradient coil and amplifier (Siemens AS25, Erlangen, Germany). The magnet and gradient system was interfaced with a spectrometer console (Varian, Palo Alto, Calif., USA) using a manufacturer-supplied interface board. Subjects were positioned supine on the patient bed above the surface coil. After coil tuning, magnetic resonance imaging was performed to determine localization for spectroscopy according to anatomical landmarks. Subjects wore earplugs to minimize gradient noise and were placed into the coil holder using cushions to minimize head movement. Shimming of the identified region of interest was performed using FASTMAP [36], which resulted in water linewidths of 7–9 Hz.

To efficiently separate the proton (169 MHz) and the ^{13}C frequency (42.5 MHz) we used a three coil design where the circular polarized ^{1}H radiofrequency (RF) field was generated by two distinct coils driven by a quadrature hybrid. The ^{13}C coil was a single loop 7 cm diameter surface coil. This three coil design was recently described elsewhere [33]. To ensure further electrical isolation to enable ^{1}H decoupling during the data acquisition, the cable feeding the ^{13}C coil was filtered using a low-pass filter and the ^{1}H RF path was filtered using a ^{1}H bandpass filter. This arrangement ensured that insertion loss prior to the first amplification stage was at most 0.2 dB [33]. Observation of the FDA guidelines for power absorption was verified using methods and procedures presented in detail elsewhere [32, 33]. RF power for excitation, polarization transfer and decoupling was carefully calibrated using a small sphere containing 0.5 ml of ^{13}C-labeled formic acid placed at the ^{13}C coil center as described previously [see 32 and references therein]. These calibrations were used to ensure proper power settings for decoupling as well as to minimize RF power needed for the experiment.

Localization was performed on the longitudinal proton z-magnetization, which was transferred to the ^{13}C magnetization using polarization transfer, PRoton Excited Carbon-13 Image SElected in vivo Localized spectroscopY, or PRECISELY [32]. For the current study, we replaced the ^{13}C part of the pulse sequence using a segmented 0° BIR-4 pulse [37]. Use of this pulse improved stability of the method in that the signal generated was much less dependent on spatial RF power precalibrations. Adiabaticity of the pulse sequence was verified using a cylindrical phantom consisting of 4-^{13}C glutamate placed into a bottle filled with a solution containing natural abundance equimolar NAA and Cr (10 mM).

Spectra were analyzed using the peak fitting software algorithm supplied by the spectrometer software. To reduce variability, peak linewidths of [13]C-^{13}C doublets were set to that of the corresponding center peak and the fitted frequencies of the [13]C-^{13}C doublets were verified to be symmetric to the main resonance.

Preliminary fitting to multiple time courses was done simultaneously analogous to a recent report [8], which permitted analysis of parameter covariance. Metabolite concentrations were assumed constant and the rate constants indicated were fitted. Fitting was based on coupled differential equations that were derived from the principle that the rate of label accumulation in a product P is given by

$$\frac{d^{13}P}{dt}(t) = \sum_i V_i^{(in)} \frac{^{13}S_i(t)}{S_i} - \sum_j V_j^{(out)} \frac{^{13}P(t)}{P} \qquad (1)$$

where it was assumed that multiple pathways (denoted by the substrates S_i and the fluxes $V_i^{(in)}$ can form the metabolite P and that multiple reactions can use P as a substrate, with the corresponding flux denoted by $V_j^{(out)}$. Note that equation 1 is specific for a given carbon nucleus in a specific molecule: For instance, α-ketoglutarate (α-KG) C4 receives label from acetyl-CoA and thus eventually from pyruvate C3, whereas α-KG C3 receives label that previously passed through α-KG C4. It is beyond the scope of this paper to present the derivation of the specific differential equations used in the calculations. Briefly, the following approach was used: (a) metabolic steady state was assumed, i.e. in equation 1 metabolite concentrations, such as S_i or P, were assumed to be constant in time, as were metabolic rates, V; (b) all metabolic intermediates of glycolysis and TCA cycle were assumed to have a small concentration relative to the metabolic rate such that their effect on the labeling kinetics was ignored in the modeling; (c) lactate was assumed to be in fast exchange with pyruvate (Pyr) and thus replaced the latter; (d) that exchange of lactate across the cell membranes was fast such that Lac represents a single kinetic pool in brain [38].

Results

The sensitivity afforded by the 4 Tesla field and by the PRECISELY pulse sequence was sufficient to measure the *natural abundance* brain glucose signal of the C2-C5 carbons in unlocalized spectra within 12 min and the concomitant measurement of the C1 resonance as shown in figure 1A. Using correction factors determined in a phantom with natural abundance glucose from the peak intensity at 76.6 ppm relative to the C1 position, the in vivo enrichment of glucose was calculated in the human brain in two studies 60 min after infusion start. The time course of plasma glucose and the brain glucose fractional enrichment, estimated from the steady-state value determined as above and then calculated from the brain ^{13}C signal divided by the plasma concentration is shown in figure 1B. The fractional enrichment achieved was highly reproducible and consistent with the increment of plasma glucose generated by the bolus method of ^{13}C glucose administration. The NMR measurement of fractional enrichment of glucose was assumed to represent fractional enrichment of brain glucose based on a relatively small contribution of blood signal (CBV is approximately 5%) and based on the observation that brain glucose signal
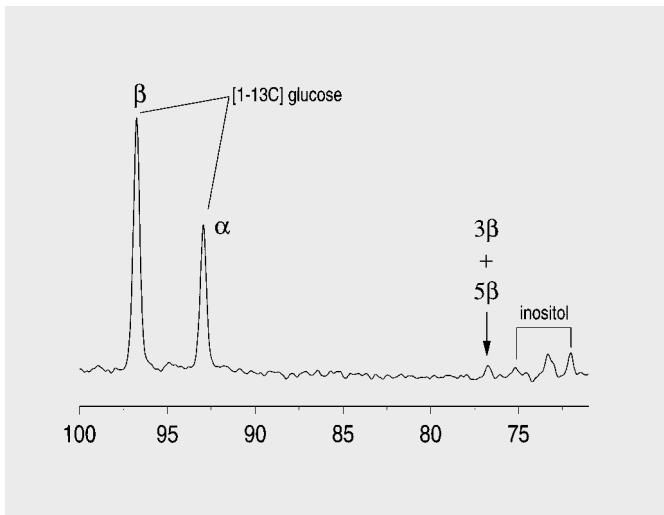
1A
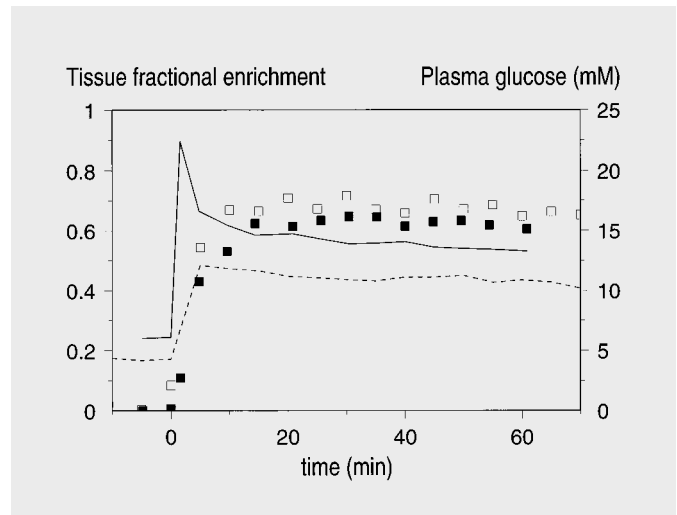
1B

Fig. 1. Direct in vivo measurement of the fractional enrichment of glucose. **A** shows the expanded spectral region covering the glucose resonances and the inositol resonances, acquired from a human head in 12 min without gradient localization. The peak at 76.6 ppm (arrow) is from the C3 and C5 of natural abundance β-*D*-glucose. The time course calculated from the calibrated ratio of 1–^{13}C tissue glucose signal to total plasma glucose is shown in **B** for two studies, indicating a highly reproducible administration of labeled glucose. The squares indicate the thus estimated brain glucose fractional enrichment (left scale) and the lines indicate the plasma glucose (right scale) during these studies. The open squares and dashed line correspond to subject 1 in table 1 and the solid squares and solid line to subject 2.

Fig. 2. Localized in vivo spectrum of the human occipital lobe. Shown is a spectrum acquired in 50 min from a 72-ml volume approximately 60 min after the start of the infusion. The top trace is an expansion of the bottom trace to highlight the observation of homonuclear ^{13}C-^{13}C coupling in the glutamate resonances and tentatively in the aspartate resonances. Processing consisted of 2 Hz Lorentz-to-Gauss resolution enhancement.
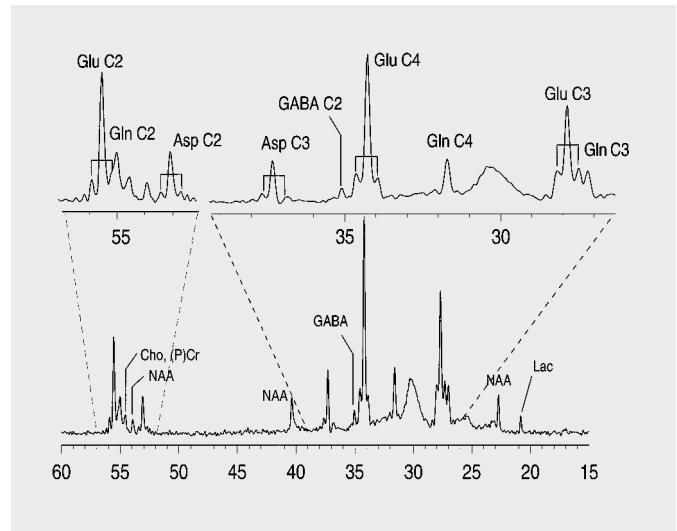
2

closely mimics that of plasma glucose [39], even when using no other localization means than the RF profile of the surface coil. Brain glucose enrichment and the concomitant increase of plasma glucose above baseline immediately following the 1-^{13}C bolus are tabulated in the first three columns of table 1. For such a short infusion time (2–5 min for bolus administration) the increment in plasma glucose produced with 99% enriched 1-^{13}C glucose allows to estimate the enrichment of plasma glucose, provided total body glucose consumption can be neglected over such a short time period.

The linewidths of glutamate ranged from 3 to 8 Hz in the in vivo spectra. A spectrum acquired 60 min after start of the infusion is shown in figure 2. The bottom

Table 1. Measurement of the increment in plasma glucose (% of baseline value, measured at t > 5–10 min) generated by a bolus injection of 99% enriched glucose, fractional enrichment measured in the brain by NMR and the doublet content of total signal intensity in glutamate; measurements are from the two studies shown in figure 1B

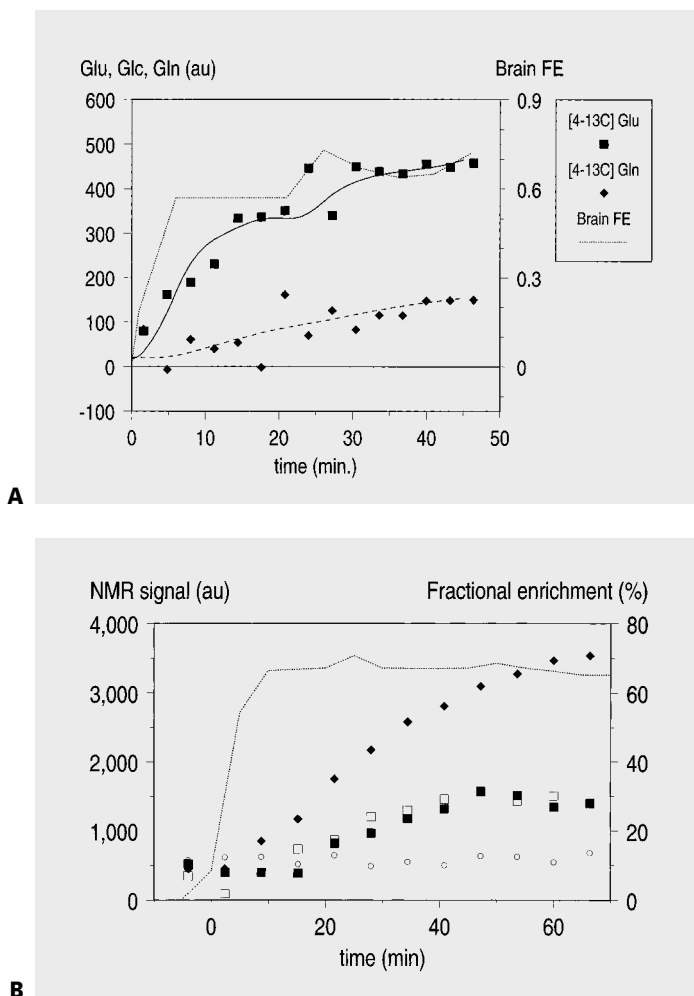|	Plasma increase	FE by NMR	C2	C4	C3
Study 1	64%	69%	22%	18%	34%
Study 2	61%	64%	20%	17%	31%

Fig. 3. Time course of the C4 (**A**) and C2 (**B**) amino acid resonances after infusion of 1–[13]C labeled glucose. In **A**, the Glu C4 (solid squares) and Gln C4 (solid diamonds) signal intensities (left scale) are plotted together with the brain glucose fractional enrichment (dotted line, right scale). The dotted line indicates the plasma glucose enrichment (right scale). The solid line and dashed line represent the best fit to this data using a model of cerebral brain metabolism (fig. 5). Note the variation in glucose fractional enrichment produced by resuming the ^{13}C glucose infusion. In **B**, the time course of the amino acid C2 resonances is shown from one subject. Note the stability of the NAA C2 peak (open circles). The closed diamonds indicate Glu C2, the open squares denote Gln C2 and the open squares Asp C2. The tissue fractional enrichment in **B** is indicated by the dotted line (right scale).

trace shows the spectral range covered by the CH_n resonances of the amino acids. Distinct resonances from Glu C2-C4, Gln C2-C4 were clearly observed in all studies. In addition, the Glu resonances contain [13]C-^{13}C doublet resonances observed as doublets at the C3 and C4 position

and as a downfield peak at the C2 position. The upfield peak of the Glu C2 [13]C-^{13}C doublet overlaps partially with the Gln C2 resonance and generates a detectable downfield shoulder at the Gln C2 position. The relative doublet content of each Glu resonance varied in concordance with the slight difference observed in the brain glucose enrichment between the two human studies shown in table 1. We tentatively observed peaks about the Asp resonances, consistent with [13]C-^{13}C doublets also being observed in Asp. The relative intensity in Asp C3 was estimated to be comparable to those observed in Glu C4.

The spectrum in figure 2 shows that the GABA C2 resonance was clearly resolved from all Glu C4 peaks. In addition, an upfield shoulder of the natural abundance aspartyl NAA peak at 40.4 ppm was tentatively observed, consistent with the chemical shift of the GABA C4 resonance. Peak intensity of GABA C2 was estimated relative to Glu and found to be on the order of 5–10% indicating a metabolically active glutamic acid decarboxylase with a participating GABA concentration on the order of 0.5 μmol/g.

We further noted that the lactate methyl peak was readily observed in the human brain and appeared to be easily labeled by ^{13}C label derived from plasma glucose (fig. 2). The intensity of this peak was estimated relative to the natural abundance NAA methyl peak at 22.7 ppm which corresponds to approximately 0.1 μmol/g ^{13}C concentration. Preliminary estimates of the minimum lactate pool size were obtained by dividing the ^{13}C lactate signal intensity by half the fractional enrichment of plasma glucose. The pool size of lactate was approximately 0.5 μmol/g which is comparable to the reported total lactate of 0.6–1 μmol/g in resting human brain [40].

Figure 3 illustrates the time course of the amino acid C2 resonances together with the NAA C2 peak. Stability of the NAA C2 signal measured at 54.0 ppm throughout this 2-hour measurement period is indicated by the open circles. Additional measurements over extended periods up to 6 h confirmed the impression that in the normal, human brain in vivo turnover of NAA may be very low. When allowing for a very conservatively estimated 100% increase in NAA signal from 0.1 to 0.2 μmol/g over 3 h, an upper limit for its turnover rate can be estimated at 0.03 μmol/g/h. Aspartate, however, labeled readily in all subjects studied. The plot in figure 3 shows that aspartate labeling leveled approximately 40 min after start of the infusion. This is consistent with malate-aspartate shuttle being the mechanism to exchange label with its partner (oxaloacetate) in the TCA cycle. Glutamate is likely to be transported by the same mechanism across

Fig. 4. Direct ^{13}C-NMR detection of label accumulation in a 22.5-ml volume encompassing the human visual cortex. **A** shows a stack plot with 3 min time resolution of the region containing the Glu C4 resonance at 34.2 ppm, **B** shows observation of less concentrated signals when extending data accumulation periods to 12 min preinfusion (bottom) and to 30 min after infusion start (top) and **C** is the plot of the Glu C4 intensity in **A**.
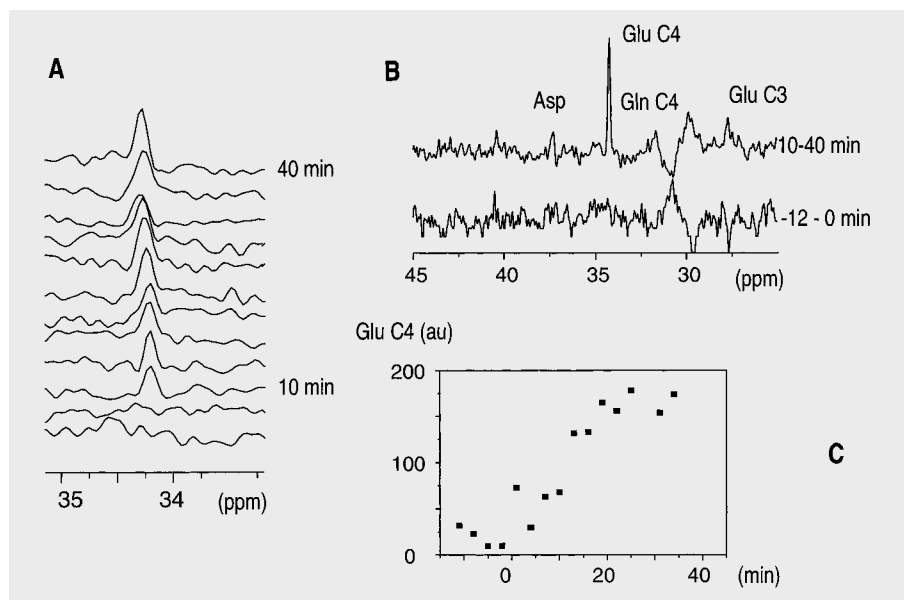
the mitochondrial membrane as part of the malate-aspartate shuttle.

A preliminary analysis indicated that labeling of Gln relative to Glu at the C2 position was 0.39 ± 0.10 (mean $\pm$ SD, n = 4) which was higher than that at the C3 position (0.18 ± 0.03, $p < 0.05$) and tentatively higher than at the C4 position (0.26 ± 0.09). Gln isotopomers not being equal to those of Glu imply that pyruvate carboxylase flux is significant in the resting human brain. The C4 of glutamine labeled somewhat more slowly than the C4 of glutamate, consistent with an earlier report [6]. However, when plotting the time course of glutamine C2 against glutamate C2 such a delay in labeling was not apparent. These preliminary observations are also consistent with a substantial pyruvate carboxylase activity.

The data presented in figures 1 and 2 sampled rather large volumes in the occipital lobe of the human brain on the order of 100 ml. To evaluate the potential to extend these measurements to areas consistently and homogenously activated by focal activation, such as the human visual cortex, we acquired a time course from a 22.5 ml ($3 \times 3 \times 2.5$ cm^3) volume centered in the primary visual cortex. The time course of the Glu C4 can be readily observed, as shown in figure 4A. Extended periods of signal accumulation permitted assessment of the labeling of other metabolites such as Gln and Asp (fig. 4B). The time course of Glu C4 corresponding to the stack plot in figure 4A is shown in figure 4C.

Discussion

The present study shows that the time course of label incorporation in vivo into cerebral glucose can be measured and that the sensitivity is sufficient to calculate in vivo fractional enrichment of glucose. Consistent results were achieved with a high enrichment of approximately 67% using a much simplified infusion protocol, as evidenced by figure 1B and table 1. To achieve a high fractional enrichment in the labeled precursor, glucose, in an economical manner, plasma glucose levels were increased in this study acutely, but modestly. Such small increases in plasma glucose are not expected to alter brain glucose metabolism rates nor transport rate constants over the time frame of the present study. Intracellular brain glucose is generally assumed not to be a regulatory factor for cerebral glucose metabolism, which is consistent with a tissue concentration well above the K_m of hexokinase in human brain at euglycemia and above [30, 31].

The present initial study further demonstrates that localized observation of ^{13}C label incorporation into all CH$_n$ groups of most major amino acids is possible in the human brain. In addition to the C4 of Gln, the C3 as well as the C2 of Gln have been easily resolved from the corresponding resonance of Glu, which represents a significant extension of previous studies [6, 25], which did not report such a capability. Labeling of the Asp C2 and C3 resonances was readily observed in the present study (fig. 2) as well as the three natural abundance CH$_n$ peaks of NAA.

The much improved sensitivity of the present study over previous reports is attributed mainly to the increased field strength as was previously documented using natural abundance ^{13}C-NMR [32]. In the present study, the higher magnetic field strength led to the in vivo observation of the GABA C2 resonance at 35.3 ppm, which may have been previously masked at lower field strength by overlap with the downfield part of the [13]C-^{13}C doublet at Glu C4. Finally, we note that label incorporation into lactate, another low concentration metabolite that is difficult to measure in the resting normal human brain even with ^{1}H-NMR spectroscopy [40–42], was readily observed in this study using ^{13}C-NMR.

From these observations, several implications for the study of human cerebral neurochemistry can be drawn: First, the apparent stability of three NAA resonances during ^{13}C infusions lasting up to 6 h suggest that in the normal human brain, the N-acetylaspartate turnover rate is below 0.03 μmol/g/h. However, this may be different under pathologic conditions and remains to be further elucidated. Second, the GABA resonance was observed at 35.3 ppm after 1-^{13}C glucose infusion which is consistent with a metabolically active pool size of 0.5–1 μmol/g in the resting human visual cortex. The GABA pool size is comparable to total GABA concentration [43, 44] which suggests a very active flux through glutamic acid decarboxylase. Third, from the observation of significant ^{13}C-labeled lactate, we conclude that in the *resting* human brain, when oxidative metabolism is tightly coupled to glycolysis [45], significant lactate metabolism is present, consistent with measurements of lactate readily crossing the blood-brain barrier [46]. This observation indicates that the necessary substrate concentration is present to drive lactate produced in glial cells to the neurons for oxidative metabolism [2]. Furthermore, the labeling of lactate from 1-^{13}C glucose suggests that plasma glucose is the major source of cerebral lactate, although it remains to be shown to what extent label incorporation occurs indirectly via, e.g., glutamate [3].

Because of the scarcity of in vivo data, few studies have attempted to model in vivo time courses. Noteworthy exceptions are the reports by Mason et al. [7] modeling single-compartment Glu C4/C3 labeling kinetics in human brain [based on data reported in 6] and including the modeling of Gln C4 turnover. However, brain metabolism is clearly multicompartmental and extract studies have recognized this fact [e.g., 5, 12, 24]. Recently, an in vivo study has included the glial compartment [25] for modeling Glu C4 and Gln C4 label accumulation. Unfortunately, the model therefore was restricted to the measurement of TCA cycle flux (from Glu C4) and to sepa-

rately calculating the rate of apparent neurotransmission (denoted in that paper flux from glutamate to glutamine, V_{gln}) from Gln C4.

The information content present in our spectra allows for additional information to be assessed. The information that can potentially be modeled based on such in vivo measurements is illustrated in figure 5. Assuming rapid lactate transport across cell membranes, the glial and neuronal Lac pools have been lumped into one kinetic pool, thus allowing for one metabolic rate for glucose consumption to be modeled. In the TCA cycle, modeling can be extended significantly over previous studies of the brain: In addition to the capability of modeling Glu and Gln C4, the respective C3 and C2 resonances can be measured, thus allowing assessment of V_{PC} and V_x. The simultaneous observation of Glu resonances and of Asp suggests that the Krebs cycle and associated exchange reactions can be studied in the human brain at a level hitherto not possible: The mitochondrial exchange rate V_x also describes the rate of exchange between Asp and oxaloacetate (OAA) and the measurement of Asp C2 and C3 is expected to further shed light on V_x. Conversely, to evaluate the use of Asp in assessing TCA cycle flux, the time course was fitted to the Asp C2 label accumulation curve. Assuming Asp = 1 μmol/g and $V_x/V_{PDH} \gg 1$ yielded for two studies $0.5*V_{PDH} = 0.37 \pm 0.08$ μmol/g/min, which was consistent with the value previously reported from Glu C4/C3 analysis under similar assumptions [7]. Fitting the model to the C4 resonances of Gln and Glu gave $0.5*V_{PDH} = 0.43 \pm 0.03$ μmol/g/min and $V_{NT}^{app} = 0.32 \pm 0.09$ μmol/g/min for the study shown in figure 3A. The model further predicts that if metabolic trafficking due to neurotransmitter release (indicated by glutamate and glutamine exchange and denoted by V_{NT}^{app} in fig. 5) is very fast compared to the glial metabolic rates, e.g. V_{PC}, the rate and extent of labeling of Gln at steady state must be identical relative to the corresponding Glu position. The increased label at the C2 of Gln relative to Glu suggests that pyruvate carboxylase activity may be significant in the resting human brain, although its contribution appears to be small. Simulations performed at t = 60 min suggested relative label in Gln C2 elevated compared to C3 by approximately 80% is consistent with $V_{PC}/V_{NT}^{app} \sim 0.25$, i.e. 0.08 μmol/g/min. This value may appear high; however, in primary cultures of adult brain and astrocytes a rate of 1.2–1.8 nmol/mg protein/min was measured [16]. More studies combined with extensive modeling are needed and planned to further delineate the accuracy of our observations. Nevertheless, since pyruvate carboxylase is localized exclusively to glia and its activity can lead

Fig. 5. Proposed modeling of ^{13}C labeling observed in the human brain. Observed metabolite pools with the corresponding labeled position in the molecule indicated by the subscript are indicated in bold type. All other metabolites are assumed to be below 0.1 µmol/g and are assumed to have a negligible effect on labeling kinetics. Enzymes are heavily compartmentalized between glial type cells and neuronal type cells, such as pyruvate carboxylase, EC 6.4.1.1, whose flux is indicated by V_{PC}, glutamine synthetase (EC 6.3.1.2, V_{syn}), glutaminase (EC 3.5.1.2, V_{NT}^{app} in neurons, V_{gase} in glia). Glu and Gln are compartmentalized as well, with Glu predominantly neuronal and Gln predominantly glial. The excess carbon skeletons produced by V_{PC} were assumed to result in Gln efflux ($V_{efflux} = V_{PC}$). The measurement of ten labeling curves (three each for Glu and Gln, two for Asp and one each for glucose and lactate) can be used to determine the following five independent metabolic rates: the apparent rate of neurotransmission V_{NT}^{app}, mitochondrial exchange rate V_x, neuronal TCA cycle rate, denoted V_{PDH}, pyruvate carboxylase, V_{PC}, and the glucose cerebral metabolic rate CMR_{glc}.

to a different label distribution in glutamine than in glutamate, these results underline the potential of localized, in vivo ^{13}C-NMR to quantitate glial metabolism in vivo, whose quantitative contribution to total brain energy metabolism remains to be defined in vivo.

The present study was performed on human brain. Nevertheless, the ^{13}C-NMR localization methods described in this paper are extendable to in vivo animal brain studies, where the unrestricted use of RF power (SAR) permits uncompromised pulse sequence performance. We conclude that the presented methods to study in vivo cerebral metabolism permit a detailed study of in vivo neurochemistry and of several biochemical reactions and pathways. These measurements should be useful in understanding in vivo brain energy metabolism as well as metabolic trafficking in the normal brain, brain development and pathophysiological states such as neurodegenerative diseases, as well as stroke, epilepsy and hepatic encephalopathy.

References

1 Van den Berg C: A model of compartmentation in mouse brain based on glucose and acetate metabolism; in Balazs E, Cremer J (eds): Metabolic Compartmentation in the Brain. London, Macmillan, 1973, pp 137–166.

2 Magistretti P, Pellerin L: Cellular mechanisms of brain energy metabolism. Relevance to functional brain imaging and to neurodegenerative disorders. Ann NY Acad Sci 1996;777:380–387.

3 Hassel B, Sonnewald U, Fonnum F: Glial-neuronal interactions as studied by cerebral metabolism of [2-^{13}C]acetate and [1-^{13}C]glucose: An ex vivo ^{13}C-NMR spectroscopic study. J Neurochem 1995;64:2773–2783.

4 Leo GC, Driscoll BF, Shank RP, Kaufman E: Analysis of [1-^{13}C]D-glucose metabolism in cultured astrocytes and neurons using nuclear magnetic resonance spectroscopy. Dev Neurosci 1993;15:282–288.

5 Lapidot A, Gopher A: Cerebral metabolic compartmentation. Estimation of glucose flux via pyruvate carboxylase/pyruvate dehydrogenase by ^{13}C-NMR isotopomer analysis of [U-^{13}C]D-glucose metabolites. J Biol Chem 1994;269:27198–27208.

6 Gruetter R, Novotny EJ, Boulware SD, Mason GF, Rothman DL, Prichard JW, Shulman RG: Localized ^{13}C-NMR spectroscopy of amino acid labeling from [1-^{13}C]D-glucose in the human brain. J Neurochem 1994;63:1377–1385.

7 Mason GF, Gruetter R, Rothman DL, Behar KL, Shulman RG, Novotny EJ: Simultaneous determination of the rates of the TCA cycle, glucose utilization, α-ketoglutarate/glutamate exchange, and glutamine synthesis in human brain by NMR. J Cereb Blood Flow Metab 1995;15:12–25.

8 Yu X, Alpert NM, Lewandowski ED: Modeling enrichment kinetics from dynamic ^{13}C-NMR spectra: Theoretical analysis and practical considerations. Am J Physiol 1997;41:C2037–C2048.

9 Shank R, Aprison M: Biochemical aspects of the neurotransmitter function of glutamate; in Filer LJ (ed): Glutamic Acid: Advances in Biochemistry and Physiology. New York, Raven Press, 1979, pp 139–150.

10 Schuldiner S, Shirvan A, Linial M: Vesicular neurotransmitter transporters: From bacteria to humans. Physiol Rev 1995;75:369–392.

11 Bachelard H, Badar-Goffer R: NMR spectroscopy in neurochemistry. J Neurochem 1993; 61:412–429.

12 Cerdan S, Kunnecke B, Seelig J: Cerebral metabolism of [1,2-^{13}C2]acetate as detected by in vivo and in vitro ^{13}C-NMR. J Biol Chem 1990; 265:12916–12926.

13 Shank RP, Leo GC, Zielke HR: Cerebral metabolic compartmentation as revealed by nuclear magnetic resonance analysis of D-[1-^{13}C]glucose metabolism. J Neurochem 1993;61:315–323.

14 Brand A, Richter-Landsberg C, Leibfritz D: Multinuclear NMR studies on the energy metabolism of glial and neuronal cells. Dev Neurosci 1993;15:289–298.

15 Martinez-Hernandez A, Bell KP, Norenberg MD: Glutamine synthetase: Glial localization in brain. Science 1976;195:1356–1358.

16 Yu A, Drejer J, Hertz L, Schousboe A: Pyruvate carboxylase activity in primary cultures of astrocytes and neurons. J Neurochem 1983;41: 1484–1487.

17 Hogstad S, Svenneby G, Torgner IA, Kvamme E, Hertz L, Schousboe A: Glutaminase in neurons and astrocytes cultured from mouse brain: Kinetic properties and effects of phosphate, glutamate, and ammonia. Neurochem Res 1988;13:383–388.

18 Pow DV, Crook DK: Direct immunocytochemical evidence for the transfer of glutamine from glial cells to neurons – use of specific antibodies directed against the d-stereoisomers of glutamate and glutamine. Neurosci 1996;70: 295–302.

19 van Zijl PCM, Rothman D: NMR studies of brain C-13-glucose uptake and metabolism – Present status. Magn Reson Imaging 1995;13: 1213–1221.

20 Rothman DL, Novotny EJ, Shulman GI, Howseman AM, Petroff OAC, Mason GF, Nixon T, Hanstock CC, Prichard JW, Shulman RG: ^{1}H-[^{13}C]NMR measurement of [4-^{13}C]glutamate. Proc Natl Acad Sci USA 1992;89: 9603–9606.

21 Pan JLW, Mason GF, Vaughan JT, Chu WJ, Zhang YT, Hetherington HP: C-13 editing of glutamate in human brain using J-refocused coherence transfer spectroscopy at 4.1 T. Magn Reson Med 1997;37:355–358.

22 Kanamori K, Ross BD, Tropp J: Selective, in vivo observation of [$^{5-15}$N]glutamine amide protons in rat brain by ^{1}H-^{15}N heteronuclear multiple-quantum-coherence transfer NMR. J Magn Reson B 1995;107:107–115.

23 Lukkarinen J, Oja JM, Turunen M, Kauppinen RA: Quantitative determination of glutamate turnover by ^{1}H-observed, ^{13}C-edited nuclear magnetic resonance spectroscopy in the cerebral cortex ex vivo: Interrelationships with oxygen consumption. Neurochem Int 1997;31:95–104.

24 Merle M, Martin M, Villegier A, Canioni P: Mathematical modelling of the citirc acid cycle for the analysis of glutamine isotopomers from cerebellar astrocytes incubated with [1(-^{13})C]glucose. Eur J Biochem 1996;239:742–751.

25 Sibson NR, Dhankhar A, Mason GF, Behar KL, Rothman DL, Shulman RG: In vivo ^{13}C NMR measurements of cerebral glutamine synthesis as evidence for glutamate-glutamine cycling. Proc Natl Acad Sci USA 1997;94: 2699–2704.

26 Sonnewald U, Therrien G, Butterworth RF: Portacaval anastomosis results in altered neuron-astrocytic metabolic trafficking of amino acids: Evidence from ^{13}C-NMR studies. J Neurochem 1996;67:1711–1717.

27 Yudkoff M, Nelson D, Daikhin Y, Erecinska M: Tricarboxylic acid cycle in rat brain synaptosomes. Fluxes and interactions with aspartate aminotransferase and malate/aspartate shuttle. J Biol Chem 1994;269:27414–27420.

28 McKenna M, Sonnewald U, Huang X, Stevenson J, Zielke H: Exogenous glutamate concentration regulates the metabolic fate of glutamate in astrocytes. J Neurochem 1996;66:386–393.

29 Beckmann N, Turkalj I, Seelig J, Keller U: ^{13}C NMR for the assessment of human brain glucose metabolism in vivo. Biochemistry 1991; 30:6362–6366.

30 Gruetter R, Novotny EJ, Boulware SD, Rothman DL, Mason GF, Shulman GI, Shulman RG, Tamborlane WV: Direct measurement of brain glucose concentrations in humans by ^{13}C NMR spectroscopy. Proc Natl Acad Sci USA 1992;89:1109–1112.

31 Gruetter R, Ugurbil K, Seaquist ER: Steady-state cerebral glucose concentrations and transport in the human brain. J Neurochem 1998; 70:397–408.

32 Gruetter R, Adriany G, Merkle H, Andersen PM: Broadband decoupled, ^{1}H localized ^{13}C MRS of the human brain at 4 Tesla. Magn Reson Med 1996;36:659–664.

33 Adriany G, Gruetter R: A half volume coil for efficient proton decoupling in humans at 4 Tesla. J Magn Reson 1997;125:178–184.

34 Seaquist ER: Comparison of arterialized venous sampling from the hand and the foot in the assessment of in vivo glucose metabolism. Metabolism 1997;46:1364–1366.

35 Seaquist ER, Pyzdrowski K, Moran A, Teuscher AU, Robertson RP: Insulin-mediated and glucose-mediated glucose uptake following hemipancreatectomy in healthy human donors. Diabetologia 1994;37:1036–1043.

36 Gruetter R: Automatic, localized in vivo adjustment of all first- and second-order shim coils. Magn Reson Med 1993;29:804–811.

37 Garwood M, Ke Y: Symmetric pulses to induce arbitrary flip angles with compensation for RF inhomogeneity and resonance offsets. J Magn Reson 1991;94:511–525.

38 McKenna MC, Tildon JT, Stevenson JH, Hopkins IB: Energy metabolism in cortical synaptic terminals from weanling and mature rat brain: Evidence for multiple compartments of tricarboxylic acid cycle activity. Dev Neurosci 1994; 16:291–300.

39 Gruetter R, Novotny EJ, Boulware SD, Rothman DL, Shulman RG: ^{1}H NMR studies of glucose transport in the human brain. J Cereb Blood Flow Metab 1996;16:427–438.

40 Prichard J, Rothman D, Novotny E, Petroff O, Kuwabara T, Avison M, Howseman A, Hanstock C, Shulman R: Lactate rise detected by ^{1}H NMR in human visual vortex during physiologic stimulation. Proc Natl Acad Sci USA 1991;88:5829–5831.

41 Frahm J, Kruger G, Merboldt KD, Kleinschmidt A: Dynamic uncoupling and recoupling of perfusion and oxidative metabolism during focal brain activation in man. Magn Reson Med 1996;35:143–148.

42 Sappey-Marinier D, Calabrese G, Fein G, Hugg JW, Biggins C, Weiner MW: Effect of photic stimulation on human visual cortex lactate and phosphates using ^{1}H and ^{31}P magnetic resonances spectroscopy. J Cereb Blood Flow Metab 1992;12:584–592.

43 Rothman DL, Petroff OAC, Behar KL, Mattson RH: Localized ^{1}H NMR measurements of GABA levels in human brain in vivo. Proc Natl Acad Sci USA 1993;90:5662–5666.

44 Mescher M, Merkle H, Kirsch J, Garwood M, Gruetter R: Simultaneous water suppression and editing in vivo. NMR Biomed 1998 (in press).

45 Fox PT, Raichle ME, Mintun MA, Dence C: Nonoxidative glucose consumption during focal physiologic neural activity. Science 1988; 241:462–464.

46 Knudsen G, Paulson O, Hertz M: Kinetic analysis of the human blood-brain barrier transport of lactate and its influence by hypercapnia. J Cereb Blood Flow Metab 1991;11:581–586.